



Cepheid distances from infrared long-baseline interferometry. III. Calibration of the surface brightness-color relations

P. Kervella, D. Bersier, D. Mourard, N. Nardetto, P. Fouqué, V. Coudé Du Foresto

► To cite this version:

P. Kervella, D. Bersier, D. Mourard, N. Nardetto, P. Fouqué, et al.. Cepheid distances from infrared long-baseline interferometry. III. Calibration of the surface brightness-color relations. *Astronomy and Astrophysics - A&A*, 2004, 428, pp.587-593. 10.1051/0004-6361:20041416 . hal-00175187

HAL Id: hal-00175187

<https://hal.science/hal-00175187>

Submitted on 23 Apr 2021

HAL is a multi-disciplinary open access archive for the deposit and dissemination of scientific research documents, whether they are published or not. The documents may come from teaching and research institutions in France or abroad, or from public or private research centers.

L'archive ouverte pluridisciplinaire **HAL**, est destinée au dépôt et à la diffusion de documents scientifiques de niveau recherche, publiés ou non, émanant des établissements d'enseignement et de recherche français ou étrangers, des laboratoires publics ou privés.

Cepheid distances from infrared long-baseline interferometry*

III. Calibration of the surface brightness-color relations

P. Kervella^{1,5}, D. Bersier², D. Mourard³, N. Nardetto³, P. Fouqué^{4,5}, and V. Coudé du Foresto¹

¹ LESIA, UMR 8109, Observatoire de Paris-Meudon, 5 place Jules Janssen, 92195 Meudon Cedex, France
e-mail: Pierre.Kervella@obspm.fr

² Space Telescope Science Institute, 3700 San Martin Drive, Baltimore, MD 21218, USA

³ GEMINI, UMR 6203, Observatoire de la Côte d'Azur, Avenue Copernic, 06130 Grasse, France

⁴ Observatoire Midi-Pyrénées, UMR 5572, 14, avenue Edouard Belin, 31400 Toulouse, France

⁵ European Southern Observatory, Alonso de Cordova 3107, Casilla 19001, Vitacura, Santiago 19, Chile

Received 4 June 2004 / Accepted 15 July 2004

Abstract. The recent VINCI/VLTI observations presented in Paper I have nearly doubled the total number of available angular diameter measurements of Cepheids. Taking advantage of the significantly larger color range covered by these observations, we derive in the present paper high precision calibrations of the surface brightness-color relations using exclusively Cepheid observations. These empirical laws make it possible to determine the distance to Cepheids through a Baade-Wesselink type technique. The least dispersed relations are based on visible-infrared colors, for instance $F_V(V - K) = -0.1336_{\pm 0.0008}(V - K) + 3.9530_{\pm 0.0006}$. The convergence of the Cepheid (this work) and dwarf star (Kervella et al. 2004c) visible-infrared surface brightness-color relations is strikingly good. The astrophysical dispersion of these relations appears to be very small, and below the present detection sensitivity.

Key words. stars: variables: Cepheids – cosmology: distance scale – stars: oscillations – techniques: interferometric

1. Introduction

The surface brightness (hereafter SB) relations link the emerging flux per solid angle unit of a light-emitting body to its color, or effective temperature. These relations are of considerable astrophysical interest for Cepheids, as a well-defined relation between a particular color index and the surface brightness can provide accurate predictions of their angular diameters. When combined with the radius curve, integrated from spectroscopic radial velocity measurements, they give access to the distance of the Cepheid (Baade-Wesselink method). This method has been applied recently to Cepheids in the LMC (Gieren et al. 2000) and in the SMC (Storm et al. 2004)

The accuracy that can be achieved in the distance estimate is conditioned for a large part by our knowledge of the SB relations. In our first paper (Kervella et al. 2004a, hereafter Paper I), we presented new interferometric measurements of seven nearby Cepheids. They complement a number of previously published measurements from several optical and infrared interferometers. We used these data in Paper II (Kervella et al. 2004b) to calibrate the Cepheid Period–Radius and Period–Luminosity relations. Nordgren et al. (2002) derived a preliminary calibration of the Cepheid visible-infrared

SB relations, based on the three stars available at that time (δ Cep, η Aql and ζ Gem). In the present Paper III, we take advantage of the nine Cepheids now resolved by interferometry to derive refined calibrations of the visible and infrared SB relations of these stars.

2. Definition of the surface brightness relations

By definition, the bolometric surface flux $f \sim L/D^2$ is linearly proportional to T_{eff}^4 , where L is the bolometric flux of the star, D its bolometric diameter and T_{eff} its effective temperature. In consequence, $F = \log f$ is a linear function of the stellar color indices, expressed in magnitudes (logarithmic scale), and SB relations can be fitted using for example the following expressions:

$$F_B = a_0(B - V)_0 + b_0 \quad (1)$$

$$F_V = a_1(V - K)_0 + b_1 \quad (2)$$

$$F_H = a_2(B - H)_0 + b_2 \quad (3)$$

where F_λ is the surface brightness. When considering a perfect blackbody curve, any color can in principle be used to obtain the SB, but in practice the linearity of the correspondence between $\log T_{\text{eff}}$ and color depends on the chosen wavelength

* Table 3 is only available in electronic form at
<http://www.edpsciences.org>

bands. The index 0 designates the dereddened magnitudes, and will be omitted in the rest of the paper. The a_i and b_i coefficients represent respectively the slopes and zero points of the different versions of the SB relation. Historically, the first calibration of the SB relation based on the $(B - V)$ index was obtained by Wesselink (1969), and the expression $F_V(V - R)$ is also known as the Barnes-Evans (B-E) relation (Barnes & Evans 1976). The relatively large intrinsic dispersion of the visible light B-E relations has led to preferring their infrared counterparts, in particular those based on the K band magnitudes ($\lambda = 2.0\text{--}2.4 \mu\text{m}$), as the color- T_{eff} relation is less affected by microturbulence and gravity effects (Laney & Stobie 1995). The surface brightness F_λ is given by the following expression (Fouqué & Gieren 1997):

$$F_\lambda = 4.2207 - 0.1 m_{\lambda_0} - 0.5 \log \theta_{\text{LD}} \quad (4)$$

where θ_{LD} is the limb darkened angular diameter, i.e. the angular size of the stellar photosphere.

3. Selected measurement sample

3.1. Interferometric observations

Following the direct measurement of the angular diameter of δ Cep achieved by Mourard et al. (1997) using the Grand Interféromètre à 2 Télescopes (GI2T), Nordgren et al. (2000) obtained the angular diameters of three additional Cepheids (η Aql, ζ Gem and α UMi) with the Navy Prototype Optical Interferometer (NPOI). These last authors also confirmed the angular diameter of δ Cep. Kervella et al. (2001) then determined the average angular size of ζ Gem, in the K band, from measurements obtained with the Fiber Linked Unit for Optical Recombination (FLUOR), installed at the Infrared Optical Telescope Array (IOTA). Simultaneously, the Palomar Testbed Interferometer (PTI) team resolved for the first time the pulsational variation of the angular diameter of ζ Gem (Lane et al. 2000) and η Aql (Lane et al. 2002). In Paper I, we have more than doubled the total number of measured Cepheids with the addition of X Sgr, W Sgr, β Dor, Y Oph and ℓ Car, and new measurements of η Aql and ζ Gem. These observations were obtained using the VLT INterferometer Commissioning Instrument (VINCI), installed at ESO's Very Large Telescope Interferometer (VLTI).

Including the peculiar first overtone Cepheid α UMi (Polaris), the number of Cepheids with measured angular diameters is presently nine. The pulsation has been resolved for five of these stars in the infrared: ζ Gem (Lane et al. 2002), W Sgr (Paper I), η Aql (Lane et al. 2002, Paper I), β Dor and ℓ Car (Paper I). The total number of independent angular diameter measurements taken into account in the present paper is 145, as compared to 59 in the previous calibration by Nordgren et al. (2002). More importantly, we now have a significantly wider range of effective temperatures, an essential factor for deriving precise values of the slopes of the SB-color relations.

To obtain a consistent sample of angular diameters, we have retained only the uniform disk (UD) values from the literature. The conversion of these model-independent measurements to limb darkened (LD) values was achieved using the

Table 1. Limb darkening corrections $k = \theta_{\text{LD}}/\theta_{\text{UD}}$ derived from the linear limb darkening coefficients determined by Claret (2000). The k_R coefficients were used for the GI2T measurements, $k_{R/I}$ for the NPOI, k_H for the PTI, and k_K for VINCI/VLTI and FLUOR/IOTA

Star	k_R	$k_{R/I}$	k_H	k_K
α UMi		1.046		
δ Cep	1.051	1.046		
X Sgr				1.020
η Aql		1.048	1.024	1.021
W Sgr				1.021
β Dor				1.023
ζ Gem		1.051	1.027	1.023
Y Oph				1.024
ℓ Car				1.026

linear LD coefficients u from Claret (2000), and the conversion formula from Hanbury Brown et al. (1974). These coefficients are broadband approximations of the Kurucz (1992) model atmospheres. They are tabulated for a grid of temperatures, metallicities and surface gravities and we have chosen the models closest to the physical properties of the stars. We have considered a uniform microturbulent velocity of 2 km s^{-1} for all stars. The conversion factors $k = \theta_{\text{LD}}/\theta_{\text{UD}}$ are given for each star in Table 1. Marengo et al. (2002, 2003) have shown that the LD properties of Cepheids can be different from those of stable stars, in particular at visible wavelengths. For the measurements obtained using the GI2T (Mourard et al. 1997) and NPOI (Nordgren et al. 2000), the LD correction is relatively large ($k = \theta_{\text{LD}}/\theta_{\text{UD}} \simeq 1.05$), and this could be the source of a bias at a level of 1 to 2% (Marengo et al. 2004). However, in the infrared the correction is much smaller ($k \simeq 1.02$), and the error on its absolute value is expected to be significantly below 1%. Considering the relatively low average precision of the currently available measurements at visible wavelengths, the potential bias due to limb darkening on the SB-color relations fit is considered negligible.

3.2. Photometric data and reddening corrections

We compiled data in the *BVRI* and *JHK* filters from different sources. Rather than try to use the largest amount of data from many different sources, we decided to limit ourselves to data sets with high internal precision, giving smooth light curves, as we wanted to fit Fourier series to the photometric data. These Fourier series were interpolated to obtain magnitudes at the phases of our interferometric measurements. The R band magnitudes were only available in sufficient number and quality for three stars: α UMi, β Dor and ℓ Car. Overall, the number of stars and photometry points per band are the following: B and V : 9 stars, 145 points; R : 3 stars, 35 points; I : 8 stars, 119 points; J : 6 stars, 127 points; H : 5 stars, 100 points; K : 8 stars, 128 points. We took the periods from Szabados (1989, 1991) to compute phases.

The *BVRI* band magnitudes are defined in the Cousins system. There is no widely used standard system in the infrared (*JHK*). We used three sources of data: Wisniewski & Johnson (1968) in the Johnson system, Laney & Stobie (1992)

in the SAAO system, and Barnes et al. (1997) in the CIT system. There is a large body of homogeneous and high quality data for Cepheids (Laney & Stobie 1992) in the SAAO system (Carter 1990). Furthermore, many stars in the list of Laney & Stobie are going to be observed with the VLTI in the near future. For convenience, we thus decided to transform all photometry into this system, using transformation relations in Glass (1985) and Carter (1990).

α UMi: For this low amplitude variable ($\Delta m_V \approx 0.1$), we considered its average photometry, as we have only an average angular diameter measurement by Nordgren et al. (2000). The B and V magnitudes were taken from the HIPPARCOS catalogue (Perryman et al. 1997), the R and I bands are from Morel & Magnenat (1978), and the K band is from Ducati (2002).

δ Cep: We used BVI data from Moffett & Barnes (1984) Barnes et al. (1997) and Kiss (1998). The JHK data of Barnes et al. (1997) have been transformed to the SAAO system.

X Sgr: Optical data come from Moffett & Barnes (1984), Berdnikov & Turner (2001a), Berdnikov & Turner (1999), Berdnikov & Turner (2000), and Berdnikov & Caldwell (2001).

η Aql: We used BVI data from Barnes et al. (1997), Kiss (1998), Berdnikov & Turner (2000), Berdnikov & Turner (2001a), Berdnikov & Caldwell (2001), and Caldwell et al. (2001). The JHK data are from Barnes et al. (1997). They have been transformed to the SAAO system using formulae given in Carter (1990).

W Sgr: We used optical data from Moffett & Barnes (1984), Berdnikov & Turner (1999), Berdnikov & Turner (2000), Berdnikov & Turner (2001a), Berdnikov & Turner (2001b), Berdnikov & Caldwell (2001), and Caldwell et al. (2001).

β Dor: We used $BVRI$ data from Berdnikov & Turner (2001a), Berdnikov & Turner (2000), Berdnikov & Turner (2001b), and Berdnikov & Caldwell (2001). In the infrared we used the data in Laney & Stobie (1992).

ζ Gem: We used BVI data from Moffett & Barnes (1984), Shobbrook (1992), Kiss (1998), Berdnikov & Turner (2001a), Berdnikov & Turner (2001b), and Berdnikov & Caldwell (2001). In the JK bands we used data from Johnson, transformed using formulae in Glass (1985).

Y Oph: In the optical we used data from Moffett & Barnes (1984) and Coulson & Caldwell (1985). In the infrared we used the data in Laney & Stobie (1992).

ℓ Car: We used $BVRI$ from Berdnikov & Turner (2001a), and Berdnikov & Turner (2000). Infrared data are from Laney & Stobie (1992).

The extinction A_λ (Table 2) was computed for each star and each band using the relations:

$$A_\lambda = R_\lambda E(B - V) \quad (5)$$

where we have (Fouqué et al. 2003; Hindsley & Bell 1989 for the R band):

$$R_B = R_V + 1 \quad (6)$$

$$R_V = 3.07 + 0.28(B - V) + 0.04 E(B - V) \quad (7)$$

$$R_R = R_V - 0.97 \quad (8)$$

Table 2. Pulsation parameters (T_0 is the Julian date of the reference epoch, P is the period in days) and color excesses (from Fernie 1990) for the Cepheids discussed in this paper. $(B - V)_0$ is the mean dereddened $(B - V)$ color as reported in the online database by Fernie et al. (1995).

Star	T_0 (JD)	P (days)	$(B - V)_0$	$E(B - V)$
α UMi	2 439 253.230	3.972676	0.598	-0.007
δ Cep	2 436 075.445	5.366341	0.657	0.092
X Sgr	2 452 723.949	7.013059	0.739	0.197
η Aql	2 445 342.479	7.176769	0.789	0.149
W Sgr	2 452 519.248	7.594904	0.746	0.111
β Dor	2 452 214.215	9.842425	0.807	0.044
ζ Gem	2 442 059.774	10.15097	0.798	0.018
Y Oph	2 452 715.481	17.12691	1.377	0.655
ℓ Car	2 452 290.416	35.55134	1.299	0.170

$$R_I = 1.82 + 0.205(B - V) + 0.0225 E(B - V) \quad (9)$$

$$R_J = R_V / 4.02 \quad (10)$$

$$R_H = R_V / 6.82 \quad (11)$$

$$R_K = R_V / 11. \quad (12)$$

4. General surface brightness relations

The data that we used for the SB-color relation fits are presented in Table 3, that is available in electronic form at <http://www.edpsciences.org/>. The limb darkened angular diameters θ_{LD} were computed from the uniform disk values available in the literature, using the conversion coefficients $k = \theta_{LD}/\theta_{UD}$ listed in Table 1. The $BVRIJHK$ magnitudes are interpolated values, corrected for interstellar extinction (see Sect. 3.2).

The resulting SB relation coefficients are presented in Table 4, and Fig. 1 shows the result for the $F_V(V - K)$ relation. The other relations based on the V band surface brightness F_V are plotted in Fig. 2. The smallest residual dispersions are obtained for the infrared-based colors, for instance:

$$F_B = -0.1199_{\pm 0.0006}(B - K) + 3.9460_{\pm 0.0007} \quad (13)$$

$$F_V = -0.1336_{\pm 0.0008}(V - K) + 3.9530_{\pm 0.0006}. \quad (14)$$

The reduced χ^2 of all the visible-infrared SB relations fits is below 1.0, meaning that the true intrinsic dispersion is undetectable at the current level of precision.

In the present paper, no error bars have been considered in the reddening corrections. This is justified by the low sensitivity of the visible-infrared SB relations to the reddening, but may create biases in the purely visible SB relations (based on the $B - V$ index for instance). However, the maximum amplitude of these biases is expected to be significantly below the residuals of the fits σ_λ listed in Table 4.

In an attempt to refine the reddening coefficients, we tentatively adjusted their values in order to minimize the dispersion of the fitted SB relations. We confirm the results of Fernie (1990) for most stars, but we find higher color excesses for

Table 4. Surface brightness relations using *BVRIJHK* based colors: $F_\lambda(C_\lambda - C_1) = a_\lambda(C_\lambda - C_1) + b_\lambda$. The 1σ errors in each coefficient are given in superscript, multiplied by 1000 to reduce the length of each line, i.e. $-0.2944^{2.4}$ stands for -0.2944 ± 0.0024 . The standard deviation of the residuals σ is listed for each SB relation, together with the reduced χ^2 of the fit and the total number of measurements N_{meas} taken into account (photometric data were unavailable for some stars).

$C_\lambda \downarrow$	$C_1 \rightarrow B$	V	R	I	J	H	K
a_B		$-0.2944^{2.4}$	$-0.1978^{1.6}$	$-0.1800^{0.9}$	$-0.1401^{0.8}$	$-0.1224^{0.7}$	$-0.1199^{0.6}$
b_B		$3.8813^{1.1}$	$3.8719^{0.9}$	$3.9283^{0.6}$	$3.9297^{0.8}$	$3.9423^{0.8}$	$3.9460^{0.7}$
$\sigma_B/\chi^2_{\text{red}}$		$0.017/1.20$	$0.008/0.46$	$0.015/1.41$	$0.015/0.65$	$0.014/0.63$	$0.015/0.75$
N_{meas}		145	34	119	127	100	128
a_V	$0.1956^{1.8}$		$-0.3789^{10.0}$	$-0.3077^{2.4}$	$-0.1759^{1.4}$	$-0.1379^{1.0}$	$-0.1336^{0.8}$
b_V	$3.8828^{0.9}$		$3.8516^{2.2}$	$3.9617^{0.7}$	$3.9407^{0.7}$	$3.9490^{0.7}$	$3.9530^{0.6}$
$\sigma_V/\chi^2_{\text{red}}$	$0.017/1.75$		$0.014/0.75$	$0.016/0.89$	$0.015/0.57$	$0.014/0.58$	$0.015/0.70$
N_{meas}		145	34	119	127	100	128
a_R	$0.0994^{1.1}$	$0.2868^{8.0}$		$-1.2894^{26.4}$	$-0.2240^{3.2}$	$-0.1458^{1.6}$	$-0.1386^{1.5}$
b_R	$3.8746^{0.6}$	$3.8554^{1.7}$		$4.3248^{2.9}$	$3.9532^{0.7}$	$3.9426^{0.6}$	$3.9430^{0.6}$
$\sigma_R/\chi^2_{\text{red}}$	$0.008/0.72$	$0.015/1.10$		$0.060/1.19$	$0.006/0.12$	$0.005/0.14$	$0.005/0.18$
N_{meas}		34	34	34	34	34	34
a_I	$0.0808^{0.6}$	$0.2105^{1.9}$	$1.8067^{38.4}$		$-0.2854^{7.1}$	$-0.1713^{2.6}$	$-0.1630^{2.0}$
b_I	$3.9304^{0.4}$	$3.9642^{0.5}$	$4.6102^{4.3}$		$3.9323^{1.7}$	$3.9491^{0.9}$	$3.9548^{0.8}$
$\sigma_I/\chi^2_{\text{red}}$	$0.015/2.23$	$0.016/1.37$	$0.089/1.35$		$0.013/0.34$	$0.010/0.40$	$0.013/0.50$
N_{meas}		119	119	34	101	74	102
a_J	$0.0399^{0.6}$	$0.0753^{1.1}$	$0.1243^{2.2}$	$0.1877^{5.3}$		$-0.2988^{10.2}$	$-0.2614^{6.8}$
b_J	$3.9295^{0.6}$	$3.9403^{0.6}$	$3.9536^{0.5}$	$3.9335^{1.2}$		$3.9679^{1.7}$	$3.9722^{1.3}$
$\sigma_J/\chi^2_{\text{red}}$	$0.015/0.89$	$0.015/0.86$	$0.006/0.20$	$0.013/0.54$		$0.015/0.21$	$0.016/0.29$
N_{meas}		127	127	34	101	100	127
a_H	$0.0223^{0.5}$	$0.0375^{0.8}$	$0.0460^{1.1}$	$0.0700^{1.8}$	$0.2060^{7.2}$		$-2.3858^{309.8}$
b_H	$3.9422^{0.6}$	$3.9487^{0.5}$	$3.9428^{0.4}$	$3.9480^{0.7}$	$3.9710^{1.2}$		$4.0653^{8.4}$
$\sigma_H/\chi^2_{\text{red}}$	$0.014/0.77$	$0.014/0.74$	$0.005/0.22$	$0.010/0.62$	$0.015/0.35$		$0.029/0.03$
N_{meas}		100	100	34	74	100	100
a_K	$0.0197^{0.5}$	$0.0331^{0.7}$	$0.0389^{1.1}$	$0.0618^{1.4}$	$0.1704^{4.7}$	$2.7121^{354.8}$	
b_K	$3.9458^{0.5}$	$3.9524^{0.5}$	$3.9435^{0.4}$	$3.9539^{0.5}$	$3.9767^{0.9}$	$4.0970^{0.6}$	
$\sigma_K/\chi^2_{\text{red}}$	$0.015/0.94$	$0.015/0.92$	$0.005/0.28$	$0.012/0.80$	$0.016/0.51$	$0.034/0.03$	
N_{meas}		128	128	34	102	127	100

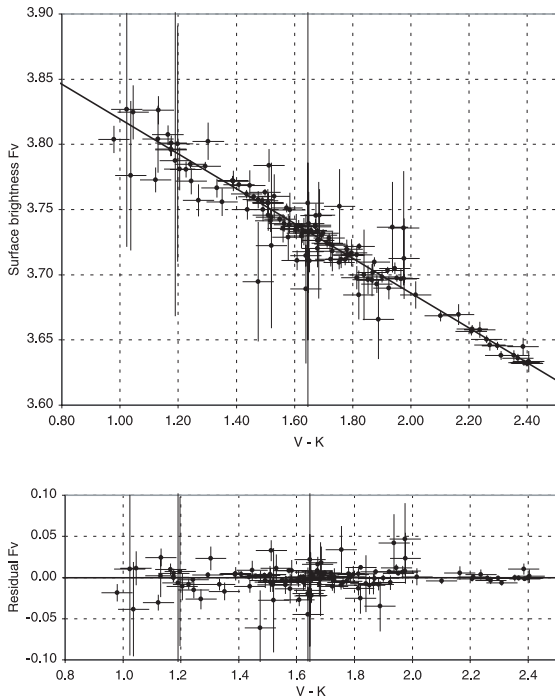


Fig. 1. Linear fit of $F_V(V - K)$ (upper part) and the corresponding residuals (lower part). The fitted coefficients are given in Table 4.

X Sgr (≈ 0.38) and W Sgr (≈ 0.29), and a slightly lower value for Y Oph (≈ 0.54). However, these numbers should be considered with caution, as our method relies on the assumption that all Cepheids follow the same SB relations. Considering that we cannot verify this hypothesis based on our data, we did not use these coefficients for the fits presented in this section.

5. Specific surface brightness relations

For ζ Gem, η Aql and ℓ Car, the pulsation is resolved with a high SNR (Paper I; Lane et al. 2002). Therefore we can derive specific SB relations over their pulsation cycle, and compare them to the global ones derived from our complete sample. In particular, the slope may be different between these Cepheids that cover a relatively broad range in terms of linear diameter and pulsation period. We have limited our comparison to the $F_V(V - K)$ relations, which give small dispersions. The best fit SB relations are the following:

– η Aql ($\sigma = 0.011$):

$$F_V = -0.1395_{\pm 0.0013} (V - K) + 3.9634_{\pm 0.0004}. \quad (15)$$

– ζ Gem ($\sigma = 0.016$):

$$F_V = -0.1098_{\pm 0.0011} (V - K) + 3.9134_{\pm 0.0002}. \quad (16)$$

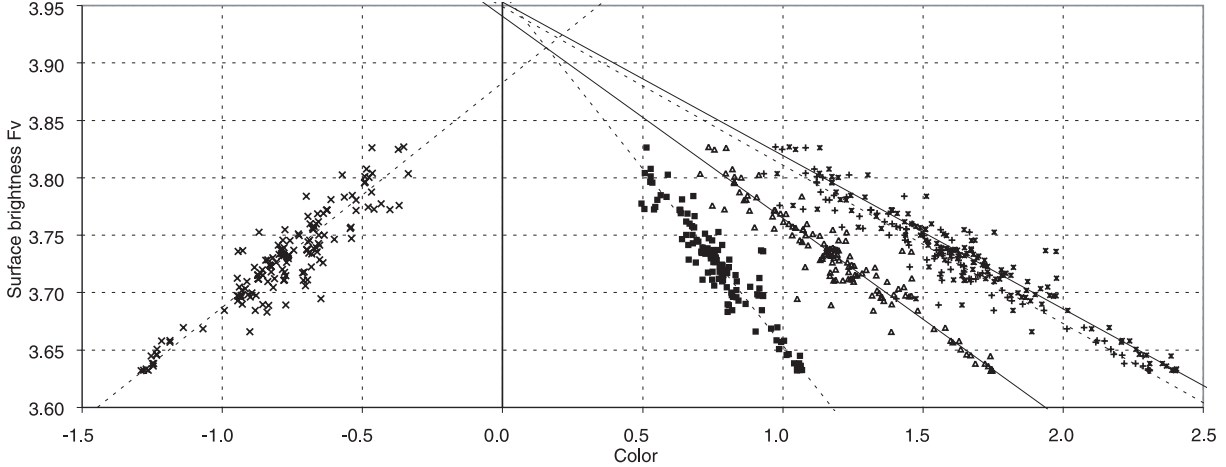


Fig. 2. Surface brightness F_V relations as a function of color. The error bars have been omitted for clarity, and the fitted models are represented alternatively as solid and dashed lines. From left to right, using the colors: $(V - B)$, $(V - I)$, $(V - J)$, $(V - H)$ and $(V - K)$. The zero-axis intersection does not happen at the same point for all relations.

– ℓ Car ($\sigma = 0.004$):

$$F_V = -0.1355_{\pm 0.0010} (V - K) + 3.9571_{\pm 0.0004}. \quad (17)$$

– All stars ($\sigma = 0.015$):

$$F_V = -0.1336_{\pm 0.0008} (V - K) + 3.9530_{\pm 0.0006}. \quad (18)$$

As shown in Fig. 3, the agreement between the extreme period η Aql ($P = 7$ days), ℓ Car ($P = 35.5$ days) and the average of all stars is good. The difference observed for ζ Gem could come from the relatively large dispersion of the measurements of this star. The poor infrared photometry available for this star could also explain part of this difference.

This result is an indication that SB-color relations for Cepheids do not depend strongly on the pulsation period of the star. Going into finer detail, it appears that the slope of the $F_V(V - K)$ relation of η Aql is slightly steeper than the slope of the same relation for ℓ Car. This could be associated with the larger surface gravity of η Aql, but the difference remains small.

6. Comparison with previous calibrations

Welch (1994) and Fouqué & Gieren (1997, FG97) proposed a calibration of the SB relations of Cepheids based on an extrapolation of the corresponding relations of giants. The latter obtained the following expression for $F_V(V - K)$:

$$F_V(\text{FG97}) = -0.131_{\pm 0.002} (V - K) + 3.947_{\pm 0.003} \quad (19)$$

to be compared with the relation we obtained in the present work:

$$F_V(V - K) = -0.1336_{\pm 0.0008} (V - K) + 3.9530_{\pm 0.0006}. \quad (20)$$

The agreement between these two independent calibrations is remarkable, with a less than 2σ difference on both the slope and the zero point.

Nordgren et al. (2002, N02) achieved a similar calibration using a larger sample of 57 stars observed with the NPOI, and

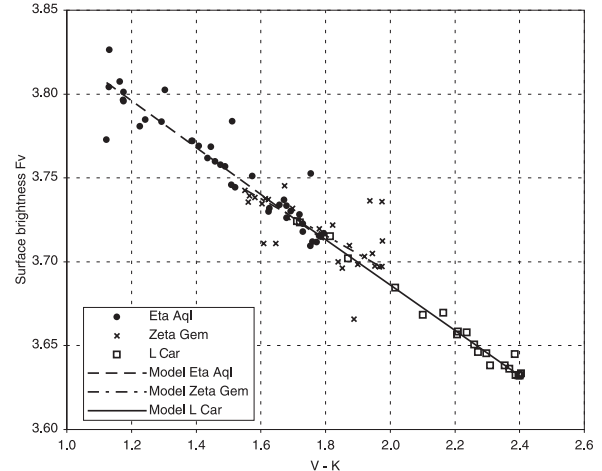


Fig. 3. Specific $F_V(V - K)$ relation fits for η Aql, ζ Gem and ℓ Car. The error bars have been omitted for clarity.

find consistent results. In addition, they compared these relations with the ones obtained from interferometric measurements of three classical Cepheids (δ Cep, η Aql, ζ Gem). They obtained:

$$F_V(\text{N02}) = -0.134_{\pm 0.005} (V - K) + 3.956_{\pm 0.011}. \quad (21)$$

This calibration is statistically identical to our result within less than 1σ , but part of the interferometric and photometric data used for the fits is common with our sample.

Several other calibrations of the SB relations for giants have been proposed in recent years, thanks to the availability of interferometric measurements. Van Belle (1999a, VB99) used a sample of 190 giants and 67 carbon stars and Miras measured with the PTI (Van Belle et al. 1999b), IOTA (e.g. Dyck et al. 1998) and lunar occultation observations (e.g. Ridgway et al. 1982) to calibrate the $F_V(V - K)$ relation of giant and supergiant stars. This author obtained an expression equivalent to:

$$F_V(\text{VB99}) = -0.112_{\pm 0.005} (V - K) + 3.886_{\pm 0.026}. \quad (22)$$

Though the slope and zero point are significantly different from our values, the maximum difference in predicted surface brightness F_V over the whole color range of the Cepheids of our sample ($1.0 \leq V - K \leq 2.4$) is less than 0.05, only twice the formal error on the zero point. The agreement is thus reasonably good.

7. Comparison with the surface brightness relations of dwarf stars

From the interferometric measurement of the angular diameters of a number of dwarfs and subgiants, Kervella et al. (2004c) calibrated the SB-color relations of these luminosity classes with high accuracy. The residual dispersion on the zero-magnitude limb darkened angular diameter was found to be below 1% for the best relations (based on visible and infrared bands). This corresponds to a dispersion in the surface brightness F of the order of 0.05% only. The metallicities [Fe/H] of the nearby dwarfs and subgiants used for these fits cover the range -0.5 to $+0.5$, but no significant trend of the SB with metallicity was detected in the visible-infrared SB relations.

The question of the universality of the SB-color relations can now be addressed by comparing the stable dwarf stars and the Cepheids. The stars of these two luminosity classes represent extremes in terms of physical properties, with for instance linear photospheric radii between 0.15 and $200 R_\odot$ and effective gravities between $\log g = 1.5$ and 5.2 , a range of three orders of magnitudes. Figure 4 shows the positions of dwarfs and Cepheids in the $F_V(B - V)$ diagram. It appears from this plot that stable dwarfs tend to have lower SB than Cepheids above $(B - V) \approx 0.8$. The difference is particularly strong in the case of ℓ Car, whose surface brightness F_V is significantly larger than that of a dwarf with the same $B - V$ color. A qualitative explanation for this difference is that for the same temperature (spectral type), giants are redder than dwarfs. This can be understood because there is more line blanketing in the supergiant atmospheres, due to their lower surface gravity and lower gas density (more ion species can exist).

Figure 5 shows the same plot for the $F_V(V - K)$ relation. In this case, the SB relations appear very close to linear for both dwarfs and Cepheids. It is almost impossible to distinguish the two populations on a statistical basis. For instance, we have:

$$F_V(\text{Dwarf}) = -0.1376_{\pm 0.0005} (V - K) + 3.9618_{\pm 0.0011} \quad (23)$$

$$F_V(\text{Ceph.}) = -0.1336_{\pm 0.0008} (V - K) + 3.9530_{\pm 0.0006}. \quad (24)$$

Over the full ($V - K$) color range of our Cepheid sample, the difference in surface brightness predicted by these relations is always:

$$F_V(\text{Dwarf}) - F_V(\text{Ceph.}) \leq 0.005. \quad (25)$$

From this remarkable convergence we conclude that the $V - K$ dereddened color index is an excellent tracer of the effective temperature. Kervella et al. (2004c) have shown that the visible- L band color indices are even more efficient than those based on the K band, and lead to extremely small intrinsic dispersions of the SB-color relations, down to ± 0.002 . High precision photometric measurements of Cepheids in the L band are

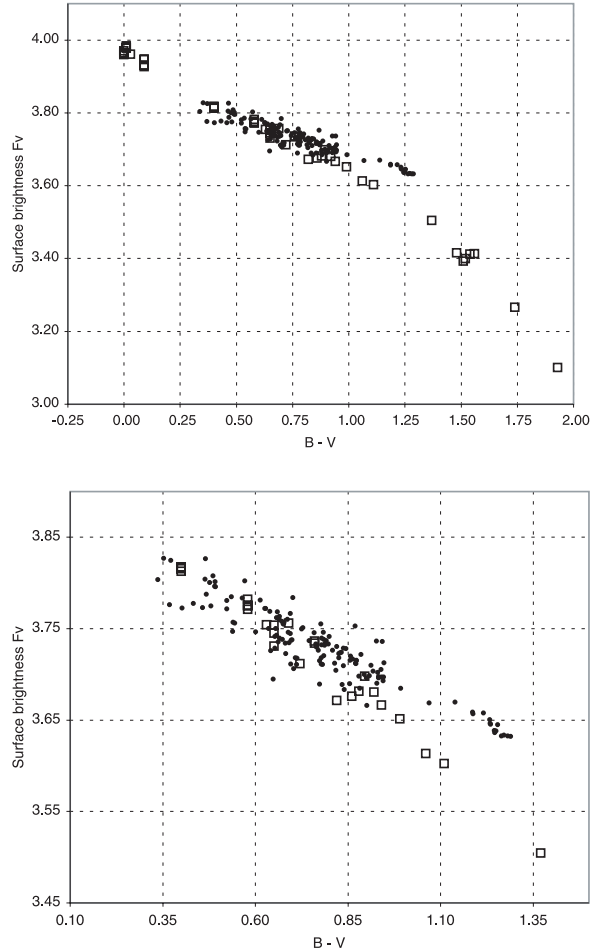


Fig. 4. Comparison of the positions of the Cepheids (solid dots) and dwarfs (open squares) in the $F_V(B - V)$ diagram. The lower part of the figure shows an enlargement of the Cepheid color range. The error bars have been omitted for clarity.

unfortunately not available at present, and we therefore recommend obtaining data in this band, to reach the smallest possible SB relation dispersions.

8. Conclusion

Taking advantage of a large sample of interferometric observations, we were able to derive precise calibrations of the SB-color relations of Cepheids. The astrophysical dispersion of the visible-infrared SB relations is undetectable at the present level of accuracy of the measurements, and could be minimal, based on the SB relations obtained for nearby dwarfs by Kervella et al. (2004c). The visible-infrared SB-color relations represent a very powerful tool for estimating the distances of Cepheids. The interferometric version of the Baade-Wesselink method that we applied in Paper I is currently limited to distances of 1–2 kpc, due to the limited length of the available baselines, but the infrared surface brightness technique can reach extragalactic Cepheids, as already demonstrated by Gieren et al. (2000) and Storm et al. (2004) for the Magellanic Clouds. The present calibration increases the level of confidence in the Cepheid distances derived by this method.

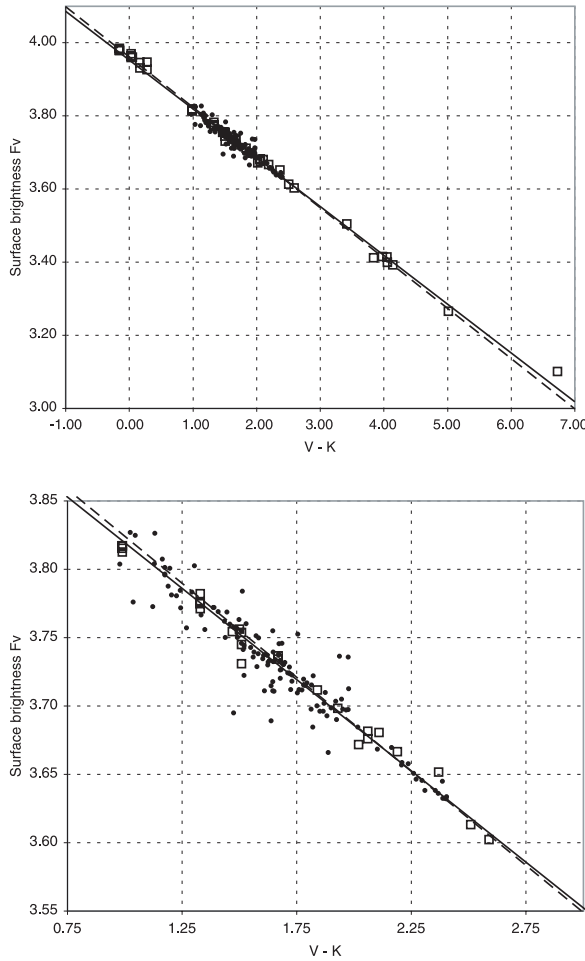


Fig. 5. Comparison of the positions of the Cepheids (solid dots) and dwarfs (open squares) in the $F_V(V - K)$ diagram. The dashed line represents the best fit SB-color relation for dwarf stars and the solid line for Cepheids. The lower part of the figure is an enlargement of the Cepheid color range.

Acknowledgements. We would like to thank Dr. Jason Aufdenberg for fruitful discussions, and we are grateful to the ESO VLT team, without whose efforts no observation would have been possible. D.B. acknowledges support from NSF grant AST-9979812. P.K. acknowledges partial support from the European Southern Observatory through a post-doctoral fellowship. Based on observations collected at the VLT Interferometer, Cerro Paranal, Chile, in the framework of the ESO shared-risk programme 071.D-0425 and an unreferenceed programme in P70. This research has made use of the SIMBAD and VIZIER databases at CDS, Strasbourg (France).

References

- Barnes, T. G., & Evans, D. S. 1976, MNRAS, 174, 489
 Barnes, T. G., III, Fernley, J. A., Frueh, M. L., et al. 1997, PASP, 109, 645
 Berdnikov, L. N., & Caldwell, J. A. R. 2001, J. Astron. Data, 7, 3
 Berdnikov, L. N., & Turner, D. G. 1999, A&A Trans., 16, 291
 Berdnikov, L. N., & Turner, D. G. 2000, A&A Trans., 18, 679
 Berdnikov, L. N., & Turner, D. G. 2001a, ApJS, 137, 209
 Berdnikov, L. N., & Turner D. G. 2001b, A&A Trans., 19, 689
 Caldwell, J. A. R., Coulson, I. M., Dean, J. F., & Berdnikov, L. N. 2001, J. Astron. Data, 7, 4
 Carter, B. S. 1990, MNRAS, 242, 1
 Claret, A. 2000, A&A, 363, 1081
 Coulson, I. M., & Caldwell, J. A. R. 1985, South African Astron. Observ. Circ., 9, 5
 Ducati, J. R. 2002, NASA Ref. Pub., 1294
 Dyck, H. M., Van Belle, G. T., & Thompson, R. R. 1998, AJ, 116, 981
 Fernie, J. D. 1990, ApJS, 72, 153
 Fernie, J. D., Beattie, B., Evans, N. R., & Seager, S. 1995, IBVS, No. 4148
 Fouqué, P., & Gieren, W. P. 1997, A&A, 320, 799
 Fouqué, P., Storm, J., & Gieren, W. 2003, Proc. Standard Candles for the Extragalactic Distance Scale, Concepción, Chile, 9–11 Dec. 2002 [arXiv:astro-ph/0301291]
 Gieren, W. P., Storm, J., Fouqué, P., Mennickent, R. E., & Gómez, M. 2000, ApJ, 533, L107
 Glass, I. S. 1985, Ir. Astr. J., 17, 1
 Hanbury Brown, R., Davis, J., Lake, J. W., & Thompson, R. J. 1974, MNRAS, 167, 475
 Hindsley, R. B., & Bell, R. A. 1989, ApJ, 341, 1004
 Kervella, P., Coudé du Foresto, V., Perrin, G., et al. 2001, A&A, 367, 876
 Kervella, P., Nardetto, N., Bersier, D., Mourard, D., & Coudé du Foresto, V. 2004a, A&A, 416, 941 (Paper I)
 Kervella, P., Bersier, D., Mourard, D., Nardetto, N., & Coudé du Foresto, V. 2004b, A&A, 423, 327 (Paper II)
 Kervella, P., Thévenin, F., Di Folco, E., & Ségransan, D. 2004c, A&A, 426, 297
 Kiss, L. L. 1998, MNRAS, 297, 825
 Kurucz, R. L. 1992, The Stellar Populations of Galaxies, IAU Symp., 149, 225
 Lane, B. F., Kuchner, M. J., Boden, A. F., Creech-Eakman, M., & Kulkarni, S. R. 2000, Nature, 407, 485
 Lane, B. F., Creech-Eakman, M., & Nordgren, T. E. 2002, ApJ, 573, 330
 Laney, C. D., & Stobie, R. S. 1992, A&AS, 93, 93
 Laney, C. D., & Stobie, R. S. 1995, MNRAS, 274, 337
 Marengo, M., Sasselov, D. D., Karovska, M., & Papaliolios, C. 2002, ApJ, 567, 1131
 Marengo, M., Karovska, M., Sasselov, D. D., et al. 2003, ApJ, 589, 968
 Marengo, M., Karovska, M., Sasselov, D. D., & Sanchez, M. 2004, ApJ, 603, 285
 Mourard, D., Bonneau, D., Koechlin, L., et al. 1997, A&A, 317, 789
 Moffett, T. J., & Barnes, T. J., III 1984, ApJS, 55, 389
 Morel, M., & Magnenat, P. 1978, A&AS, 34, 477
 Nordgren, T. E., Armstrong, J. T., Germain, M. E., et al. 2000, ApJ, 543, 972
 Nordgren, T. E., Lane, B. F., Hindsley, R. B., & Kervella, P. 2002, AJ, 123, 3380
 Perryman, M. A. C., Lindegren, L., Kovalevsky, J., et al. 1997, The HIPPARCOS Catalogue, A&A, 323, 49
 Ridgway, S. T., Jacoby, G. H., Joyce, R. R., & Wells, D. C. 1982, AJ, 87, 1044
 Shobbrook, R. R. 1992, MNRAS, 255, 486
 Storm, J., Carney, B. W., Gieren, W. P., et al. 2004, A&A, 415, 531
 Szabados, L. 1989, Comm. Konkoly Obs., 94, 1
 Szabados, L. 1991, Comm. Konkoly Obs., 96, 1
 Van Belle, G. T. 1999a, PASP, 111, 1515
 Van Belle, G. T., Lane, B. F., Thompson, R. R., et al. 1999b, AJ, 117, 521
 Welch, D. L. 1994, AJ, 108, 1421
 Wesselink, A. J. 1969, MNRAS, 144, 297
 Wisniewski, W. Z., & Johnson, H. L. 1968, Commun. Lunar Planet. Lab., 7, 57

Online Material

Table 3. Interferometric and photometric data used in the present paper. The references for the interferometric measurements are: Nordgren et al. (2000, N00), Mourard et al. (1997, M97), Nordgren et al. (2002, N02), Lane et al. (2002, L02), and Kervella et al. (2004a, K04). JD is the Julian date of the measurement, λ the interferometric measurement wavelength (in μm), ϕ the phase, θ_{UD} the uniform disk and θ_{LD} the limb darkened angular diameters (in mas). The magnitudes are corrected for interstellar extinction (see Sect. 3.2).

Star	Ref.	JD	λ	ϕ	θ_{LD}	B_0	V_0	R_0	I_0	J_0	H_0	K_0
α UMi	N00	avg	0.74	avg	3.284 ± 0.021	2.66	1.99	1.55	1.23	–	–	0.49
δ Cep	M97	2 449 566.6000	0.67	0.032	1.376 ± 0.620	3.60	3.25	–	–	2.51	2.27	2.22
δ Cep	M97	2 449 572.5000	0.67	0.132	1.534 ± 0.767	3.87	3.40	–	–	2.56	2.27	2.21
δ Cep	M97	2 449 642.3000	0.67	0.139	1.440 ± 0.567	3.89	3.41	–	–	2.56	2.27	2.21
δ Cep	M97	2 449 643.3000	0.67	0.325	2.070 ± 0.431	4.33	3.68	–	–	2.63	2.28	2.21
δ Cep	M97	2 449 541.6000	0.67	0.374	1.776 ± 0.504	4.42	3.74	–	–	2.66	2.28	2.22
δ Cep	M97	2 449 569.5000	0.67	0.573	1.660 ± 0.504	4.71	3.93	–	–	2.76	2.36	2.28
δ Cep	M97	2 449 570.5000	0.67	0.759	1.324 ± 0.841	4.83	4.05	–	–	2.87	2.49	2.40
δ Cep	M97	2 449 640.3000	0.67	0.766	1.797 ± 0.462	4.82	4.04	–	–	2.87	2.49	2.40
δ Cep	M97	2 449 571.5000	0.67	0.945	1.671 ± 0.431	3.70	3.33	–	–	2.58	2.34	2.30
δ Cep	N02	2 450 788.6300	0.74	0.754	1.621 ± 0.063	4.83	4.05	–	–	2.87	2.48	2.40
δ Cep	N02	2 450 994.9100	0.74	0.193	1.705 ± 0.094	4.02	3.48	–	–	2.58	2.27	2.21
δ Cep	N02	2 450 995.9300	0.74	0.383	1.485 ± 0.115	4.44	3.75	–	–	2.66	2.29	2.22
δ Cep	N02	2 450 996.9700	0.74	0.577	1.548 ± 0.220	4.71	3.94	–	–	2.76	2.37	2.29
δ Cep	N02	2 450 997.9300	0.74	0.756	1.422 ± 0.115	4.83	4.05	–	–	2.87	2.48	2.40
δ Cep	N02	2 450 998.9300	0.74	0.942	1.328 ± 0.125	3.72	3.35	–	–	2.59	2.35	2.30
δ Cep	N02	2 451 007.9600	0.74	0.625	1.590 ± 0.105	4.78	4.00	–	–	2.81	2.40	2.32
δ Cep	N02	2 451 008.9200	0.74	0.804	1.391 ± 0.084	4.72	3.99	–	–	2.86	2.49	2.41
δ Cep	N02	2 451 009.9600	0.74	0.998	1.548 ± 0.073	3.56	3.22	–	–	2.52	2.29	2.24
δ Cep	N02	2 451 010.9200	0.74	0.177	1.610 ± 0.073	3.98	3.46	–	–	2.57	2.27	2.21
δ Cep	N02	2 451 011.9100	0.74	0.361	1.537 ± 0.073	4.40	3.72	–	–	2.65	2.28	2.21
δ Cep	N02	2 451 012.9000	0.74	0.546	1.569 ± 0.073	4.66	3.90	–	–	2.73	2.34	2.27
δ Cep	N02	2 451 088.8100	0.74	0.691	1.380 ± 0.125	4.83	4.05	–	–	2.85	2.45	2.36
δ Cep	N02	2 451 089.7800	0.74	0.872	1.527 ± 0.073	4.27	3.73	–	–	2.76	2.44	2.38
δ Cep	N02	2 451 093.7600	0.74	0.614	1.475 ± 0.021	4.77	3.98	–	–	2.80	2.39	2.31
δ Cep	N02	2 451 097.7800	0.74	0.363	1.537 ± 0.052	4.40	3.72	–	–	2.65	2.28	2.21
δ Cep	N02	2 451 098.8500	0.74	0.562	1.694 ± 0.063	4.69	3.92	–	–	2.75	2.36	2.28
X Sgr	K04	2 452 741.9033	2.18	0.560	1.487 ± 0.058	4.88	4.17	–	3.44	–	–	–
X Sgr	K04	2 452 742.8848	2.18	0.700	1.541 ± 0.067	4.91	4.21	–	3.45	–	–	–
X Sgr	K04	2 452 743.8965	2.18	0.844	1.443 ± 0.065	4.48	3.94	–	3.20	–	–	–
X Sgr	K04	2 452 744.8676	2.18	0.983	1.489 ± 0.059	4.02	3.62	–	3.08	–	–	–
X Sgr	K04	2 452 747.8477	2.18	0.408	1.528 ± 0.217	4.65	4.00	–	3.34	–	–	–
X Sgr	K04	2 452 749.8324	2.18	0.691	1.457 ± 0.104	4.92	4.21	–	3.46	–	–	–
X Sgr	K04	2 452 766.8110	2.18	0.112	1.420 ± 0.078	4.18	3.70	–	3.15	–	–	–
X Sgr	K04	2 452 768.8768	2.18	0.406	1.441 ± 0.032	4.65	4.00	–	3.34	–	–	–
η Aql	N02	2 450 638.8600	0.74	0.990	1.959 ± 0.084	3.48	3.02	–	2.51	2.23	1.95	1.90
η Aql	N02	2 450 640.8800	0.74	0.271	1.781 ± 0.094	3.93	3.27	–	2.61	2.26	1.89	1.82
η Aql	N02	2 450 641.8600	0.74	0.408	1.938 ± 0.084	4.24	3.47	–	2.73	2.33	1.93	1.85
η Aql	N02	2 450 997.8300	0.74	0.008	1.697 ± 0.199	3.48	3.02	–	2.51	2.22	1.94	1.89
η Aql	N02	2 450 998.8800	0.74	0.154	1.781 ± 0.063	3.86	3.23	–	2.60	2.26	1.92	1.84
η Aql	N02	2 451 007.8800	0.74	0.408	1.917 ± 0.063	4.24	3.47	–	2.73	2.33	1.93	1.85
η Aql	N02	2 451 008.9100	0.74	0.552	1.603 ± 0.210	4.53	3.66	–	2.89	2.43	1.99	1.90
η Aql	N02	2 451 009.8500	0.74	0.683	1.771 ± 0.084	4.66	3.80	–	3.00	2.51	2.08	2.00
η Aql	N02	2 451 010.8400	0.74	0.821	1.456 ± 0.084	4.25	3.55	–	2.87	2.49	2.12	2.04
η Aql	N02	2 451 011.8400	0.74	0.960	1.509 ± 0.073	3.52	3.05	–	2.54	2.25	1.97	1.92
η Aql	N02	2 451 012.8700	0.74	0.104	1.603 ± 0.105	3.73	3.16	–	2.57	2.24	1.92	1.86
η Aql	L02	2 452 065.4200	1.64	0.764	1.694 ± 0.011	4.53	3.73	–	2.98	2.53	2.13	2.05
η Aql	L02	2 452 066.4140	1.64	0.903	1.694 ± 0.017	3.75	3.22	–	2.65	2.34	2.03	1.97
η Aql	L02	2 452 067.4050	1.64	0.041	1.735 ± 0.041	3.54	3.05	–	2.52	2.22	1.93	1.87
η Aql	L02	2 452 075.3830	1.64	0.153	1.783 ± 0.028	3.86	3.23	–	2.60	2.26	1.92	1.85
η Aql	L02	2 452 076.3840	1.64	0.292	1.843 ± 0.014	3.95	3.28	–	2.61	2.26	1.89	1.82
η Aql	L02	2 452 077.3720	1.64	0.430	1.867 ± 0.022	4.30	3.51	–	2.76	2.35	1.94	1.86
η Aql	L02	2 452 089.3500	1.64	0.099	1.757 ± 0.019	3.71	3.15	–	2.56	2.24	1.92	1.86

Table 3. continued.

Star	Ref.	JD	λ	ϕ	θ_{LD}	B_0	V_0	R_0	I_0	J_0	H_0	K_0
η Aql	L02	2 452 090.3540	1.64	0.239	1.842 ± 0.020	3.92	3.26	—	2.61	2.26	1.90	1.83
η Aql	L02	2 452 091.3460	1.64	0.377	1.807 ± 0.023	4.14	3.41	—	2.69	2.30	1.92	1.84
η Aql	L02	2 452 095.3600	1.64	0.936	1.605 ± 0.050	3.59	3.10	—	2.58	2.28	1.99	1.94
η Aql	L02	2 452 099.3370	1.64	0.490	1.844 ± 0.026	4.44	3.60	—	2.83	2.40	1.97	1.88
η Aql	L02	2 452 101.3290	1.64	0.768	1.672 ± 0.038	4.51	3.72	—	2.97	2.53	2.13	2.05
η Aql	L02	2 452 103.2930	1.64	0.042	1.697 ± 0.041	3.54	3.05	—	2.52	2.22	1.93	1.87
η Aql	L02	2 452 105.3000	1.64	0.321	1.842 ± 0.025	3.99	3.31	—	2.63	2.27	1.90	1.82
η Aql	L02	2 452 106.2830	1.64	0.458	1.860 ± 0.016	4.38	3.56	—	2.79	2.37	1.95	1.86
η Aql	L02	2 452 107.3020	1.64	0.600	1.853 ± 0.028	4.59	3.71	—	2.93	2.46	2.02	1.93
η Aql	L02	2 452 108.3080	1.64	0.740	1.744 ± 0.033	4.60	3.77	—	3.00	2.54	2.13	2.04
η Aql	L02	2 452 116.2760	1.64	0.851	1.650 ± 0.024	4.07	3.43	—	2.79	2.44	2.09	2.02
η Aql	K04	2 452 524.5643	2.18	0.741	1.782 ± 0.124	4.60	3.77	—	3.00	2.54	2.13	2.04
η Aql	K04	2 452 557.5462	2.18	0.336	1.916 ± 0.105	4.03	3.34	—	2.64	2.28	1.90	1.83
η Aql	K04	2 452 559.5346	2.18	0.614	1.843 ± 0.045	4.60	3.73	—	2.94	2.46	2.03	1.94
η Aql	K04	2 452 564.5321	2.18	0.310	1.846 ± 0.053	3.97	3.30	—	2.62	2.26	1.89	1.82
η Aql	K04	2 452 565.5155	2.18	0.447	1.910 ± 0.032	4.35	3.54	—	2.78	2.36	1.95	1.86
η Aql	K04	2 452 566.5185	2.18	0.587	1.900 ± 0.034	4.57	3.70	—	2.92	2.45	2.01	1.92
η Aql	K04	2 452 567.5232	2.18	0.727	1.839 ± 0.040	4.63	3.79	—	3.00	2.54	2.12	2.04
η Aql	K04	2 452 573.5114	2.18	0.561	1.923 ± 0.057	4.54	3.67	—	2.90	2.43	2.00	1.91
η Aql	K04	2 452 769.9372	2.18	0.931	1.681 ± 0.031	3.61	3.12	—	2.59	2.29	2.00	1.95
η Aql	K04	2 452 770.9222	2.18	0.068	1.828 ± 0.049	3.61	3.09	—	2.54	2.23	1.92	1.86
η Aql	K04	2 452 772.8988	2.18	0.343	1.919 ± 0.051	4.04	3.35	—	2.65	2.28	1.90	1.83
W Sgr	K04	2 452 743.8373	2.18	0.571	1.438 ± 0.103	5.43	4.59	—	3.78	—	—	—
W Sgr	K04	2 452 744.9149	2.18	0.713	1.319 ± 0.094	5.55	4.72	—	3.91	—	—	—
W Sgr	K04	2 452 749.8676	2.18	0.365	1.289 ± 0.147	5.00	4.32	—	3.59	—	—	—
W Sgr	K04	2 452 751.8659	2.18	0.628	1.348 ± 0.179	5.52	4.66	—	3.86	—	—	—
W Sgr	K04	2 452 763.8884	2.18	0.211	1.311 ± 0.035	4.75	4.15	—	3.51	—	—	—
W Sgr	K04	2 452 764.8766	2.18	0.341	1.383 ± 0.030	4.88	4.24	—	3.55	—	—	—
W Sgr	K04	2 452 765.8802	2.18	0.473	1.341 ± 0.033	5.24	4.46	—	3.71	—	—	—
W Sgr	K04	2 452 767.8671	2.18	0.735	1.234 ± 0.083	5.52	4.71	—	3.91	—	—	—
W Sgr	K04	2 452 769.9137	2.18	0.005	1.266 ± 0.064	4.35	3.92	—	3.42	—	—	—
β Dor	K04	2 452 215.7953	2.18	0.161	1.884 ± 0.082	4.21	3.46	3.13	2.73	2.30	1.91	1.86
β Dor	K04	2 452 216.7852	2.18	0.261	1.999 ± 0.048	4.40	3.58	3.22	2.80	2.34	1.92	1.86
β Dor	K04	2 452 247.7611	2.18	0.408	1.965 ± 0.060	4.76	3.81	3.42	2.97	2.45	1.99	1.93
β Dor	K04	2 452 308.6448	2.18	0.594	1.886 ± 0.076	4.73	3.85	3.46	3.03	2.53	2.11	2.04
β Dor	K04	2 452 567.8272	2.18	0.927	1.834 ± 0.063	4.02	3.39	3.09	2.73	2.35	2.01	1.95
β Dor	K04	2 452 744.5645	2.18	0.884	1.770 ± 0.072	4.12	3.47	3.16	2.79	2.39	2.03	1.98
β Dor	K04	2 452 749.5139	2.18	0.387	1.965 ± 0.110	4.71	3.78	3.39	2.95	2.43	1.98	1.91
β Dor	K04	2 452 750.5111	2.18	0.488	1.907 ± 0.076	4.83	3.91	3.48	3.04	2.52	2.05	1.98
β Dor	K04	2 452 751.5186	2.18	0.591	1.999 ± 0.172	4.74	3.86	3.47	3.04	2.53	2.10	2.04
ζ Gem	N02	2 451 098.9800	0.74	0.477	1.566 ± 0.221	5.06	4.11	—	3.19	2.65	—	2.13
ζ Gem	N02	2 451 229.8300	0.74	0.368	1.461 ± 0.231	4.95	4.02	—	3.10	2.59	—	2.08
ζ Gem	N02	2 451 232.7200	0.74	0.652	1.619 ± 0.053	4.82	3.96	—	3.18	2.67	—	2.18
ζ Gem	N02	2 451 233.7100	0.74	0.750	1.514 ± 0.063	4.61	3.85	—	3.10	2.63	—	2.18
ζ Gem	L02	2 451 605.2260	1.64	0.349	1.720 ± 0.015	4.91	4.00	—	3.08	2.58	—	2.08
ζ Gem	L02	2 451 206.2410	1.64	0.044	1.719 ± 0.048	4.32	3.65	—	2.92	2.48	—	2.07
ζ Gem	L02	2 451 214.1920	1.64	0.827	1.845 ± 0.062	4.46	3.77	—	3.05	2.58	—	2.16
ζ Gem	L02	2 451 615.1800	1.64	0.330	1.783 ± 0.032	4.88	3.97	—	3.06	2.57	—	2.07
ζ Gem	L02	2 451 617.1670	1.64	0.525	1.629 ± 0.029	5.04	4.10	—	3.21	2.67	—	2.15
ζ Gem	L02	2 451 618.1430	1.64	0.622	1.575 ± 0.008	4.89	4.00	—	3.19	2.67	—	2.18
ζ Gem	L02	2 451 619.1680	1.64	0.723	1.590 ± 0.018	4.67	3.88	—	3.12	2.64	—	2.18
ζ Gem	L02	2 451 620.1690	1.64	0.821	1.627 ± 0.029	4.47	3.77	—	3.06	2.58	—	2.16
ζ Gem	L02	2 451 622.1980	1.64	0.021	1.717 ± 0.047	4.30	3.64	—	2.93	2.48	—	2.07
ζ Gem	L02	2 451 643.1610	1.64	0.086	1.707 ± 0.012	4.37	3.68	—	2.91	2.48	—	2.05
ζ Gem	L02	2 451 981.1820	1.64	0.386	1.730 ± 0.014	4.98	4.04	—	3.12	2.60	—	2.09
ζ Gem	L02	2 451 982.1640	1.64	0.482	1.679 ± 0.021	5.06	4.11	—	3.20	2.65	—	2.13

Table 3. continued.

Star	Ref.	JD	λ	ϕ	θ_{LD}	B_0	V_0	R_0	I_0	J_0	H_0	K_0
ζ Gem	L02	2 451 983.2010	1.64	0.584	1.631 ± 0.022	4.96	4.05	—	3.21	2.67	—	2.17
ζ Gem	L02	2 451 894.3870	1.64	0.835	1.662 ± 0.020	4.45	3.76	—	3.05	2.57	—	2.16
ζ Gem	L02	2 451 895.3690	1.64	0.932	1.672 ± 0.014	4.32	3.66	—	2.98	2.52	—	2.11
ζ Gem	K04	2 452 214.8787	2.18	0.408	1.715 ± 0.059	5.01	4.07	—	3.14	2.62	—	2.10
ζ Gem	K04	2 452 216.8357	2.18	0.600	1.751 ± 0.088	4.93	4.03	—	3.21	2.67	—	2.18
ζ Gem	K04	2 451 527.9722	2.12	0.739	1.643 ± 0.334	4.63	3.86	—	3.11	2.63	—	2.18
ζ Gem	K04	2 451 601.8285	2.12	0.014	1.748 ± 0.086	4.30	3.64	—	2.93	2.48	—	2.08
ζ Gem	K04	2 451 259.7790	2.12	0.318	2.087 ± 0.291	4.85	3.95	—	3.05	2.57	—	2.06
ζ Gem	K04	2 451 262.7400	2.12	0.610	1.730 ± 0.273	4.91	4.02	—	3.20	2.67	—	2.18
ζ Gem	K04	2 451 595.8520	2.12	0.426	1.423 ± 0.284	5.03	4.08	—	3.15	2.63	—	2.11
ζ Gem	K04	2 451 602.7640	2.12	0.107	1.910 ± 0.216	4.40	3.69	—	2.91	2.48	—	2.05
Y Oph	K04	2 452 742.9056	2.18	0.601	1.462 ± 0.120	4.93	4.10	3.86	3.29	2.96	2.58	2.52
Y Oph	K04	2 452 750.8842	2.18	0.067	1.414 ± 0.106	4.26	3.64	3.50	3.00	2.77	2.49	2.44
Y Oph	K04	2 452 772.8308	2.18	0.349	1.478 ± 0.057	4.75	3.95	3.72	3.16	2.86	2.50	2.43
Y Oph	K04	2 452 786.8739	2.18	0.168	1.436 ± 0.046	4.45	3.76	3.59	3.07	2.79	2.48	2.42
ℓ Car	K04	2 452 453.4978	2.18	0.587	3.035 ± 0.109	4.73	3.46	2.89	2.41	1.72	1.16	1.06
ℓ Car	K04	2 452 739.5644	2.18	0.634	2.859 ± 0.084	4.73	3.48	2.91	2.42	1.74	1.19	1.09
ℓ Car	K04	2 452 740.5691	2.18	0.662	2.954 ± 0.046	4.72	3.47	2.92	2.42	1.75	1.22	1.12
ℓ Car	K04	2 452 741.7171	2.18	0.694	2.969 ± 0.038	4.71	3.46	2.93	2.42	1.77	1.24	1.15
ℓ Car	K04	2 452 742.7009	2.18	0.722	2.874 ± 0.054	4.69	3.45	2.94	2.43	1.80	1.27	1.18
ℓ Car	K04	2 452 743.6985	2.18	0.750	2.737 ± 0.073	4.66	3.44	2.94	2.44	1.81	1.30	1.21
ℓ Car	K04	2 452 744.6336	2.18	0.776	2.769 ± 0.033	4.62	3.43	2.92	2.43	1.82	1.31	1.22
ℓ Car	K04	2 452 745.6285	2.18	0.804	2.652 ± 0.095	4.53	3.39	2.88	2.41	1.81	1.32	1.23
ℓ Car	K04	2 452 746.6198	2.18	0.832	2.749 ± 0.045	4.40	3.33	2.81	2.37	1.79	1.31	1.23
ℓ Car	K04	2 452 747.5988	2.18	0.860	2.674 ± 0.125	4.22	3.23	2.73	2.30	1.74	1.29	1.21
ℓ Car	K04	2 452 749.5763	2.18	0.915	2.620 ± 0.076	3.82	2.96	2.53	2.13	1.63	1.23	1.15
ℓ Car	K04	2 452 751.5785	2.18	0.972	2.726 ± 0.032	3.62	2.79	2.40	2.01	1.54	1.15	1.08
ℓ Car	K04	2 452 755.6166	2.18	0.085	2.942 ± 0.110	3.78	2.85	2.44	2.01	1.51	1.06	0.98
ℓ Car	K04	2 452 763.5551	2.18	0.309	3.157 ± 0.032	4.31	3.13	2.63	2.15	1.53	1.01	0.92
ℓ Car	K04	2 452 765.5545	2.18	0.365	3.175 ± 0.033	4.43	3.19	2.69	2.21	1.56	1.02	0.93
ℓ Car	K04	2 452 766.5497	2.18	0.393	3.173 ± 0.033	4.48	3.25	2.72	2.23	1.57	1.04	0.95
ℓ Car	K04	2 452 768.5663	2.18	0.450	3.155 ± 0.036	4.60	3.35	2.78	2.29	1.62	1.07	0.98
ℓ Car	K04	2 452 769.5746	2.18	0.478	3.155 ± 0.021	4.65	3.39	2.81	2.32	1.64	1.08	1.00
ℓ Car	K04	2 452 770.5353	2.18	0.505	3.124 ± 0.021	4.69	3.41	2.84	2.35	1.66	1.10	1.01
ℓ Car	K04	2 452 771.5281	2.18	0.533	3.100 ± 0.019	4.72	3.43	2.86	2.38	1.69	1.12	1.03
ℓ Car	K04	2 452 786.6200	2.18	0.957	2.700 ± 0.064	3.64	2.82	2.42	2.03	1.56	1.17	1.09